Isospin effects on reaction dynamics at Fermi energies

Giuseppe Politi[1,2*], *Luis* Acosta[3], *Maria Victoria* Andrés[4], *Lucrezia* Auditore[1,5], *Christian* Beck[6], *Tomasz* Cap[7], *Giuseppe* Cardella[2], *Francesco* Catara[1,2], *Maria* Colonna[8], *Enrico* De Filippo[2], *Antonio* D'Onofrio[9,10], *Elena* Geraci[1,2], *Brunilde* Gnoffo[1,2], *Shuhrat* Kalandarov[11], *Marco* La Commara[9,10], *Edoardo G.* Lanza[2], *Gaetano* Lanzalone[8,12], *Concettina* Maiolino[8], *Nunzia Simona* Martorana[1,8], *Angelo* Pagano[3], *Emanuele Vincenzo* Pagano[1,8], *Massimo* Papa[3], *Erik* Piasecki[13], *Sara* Pirrone[3], *Lucia* Quattrocchi[1,2], *Francesca* Rizzo[1,8], *Paolo* Russotto[8], *Domenico* Santonocito[8], *Krystyna* Siwek-Wilczynska[14], *Antonio* Trifirò[2,5], *Marina* Trimarchi[2,5], and *Andrea* Vitturi[15].

[1]Dipartimento di Fisica e Astronomia, Università di Catania, Catania, Italy
[2]Istituto Nazionale di Fisica Nucleare - Sezione di Catania, Catania, Italy
[3]Instituto de Fisica, Universidad Nacional Autonoma de Mexico, Mexico City, Mexico
[4]Departamento de FAMN, Universidad de Sevilla, Sevilla, Spain
[5]Dipartimento di Scienze Matematiche e Informatiche, Scienze Fisiche e Scienze della Terra, Università di Messina, Messina, Italy
[6]Institut Pluridisciplinaire Hubert Curien, Université de Strasbourg, CNRS-IN2P3, UMR7178, Strasbourg, France
[7]National Centre for Nuclear Research, Otwork-Swierk, Poland
[8]Istituto Nazionale di Fisica Nucleare - Laboratori Nazionali del Sud, Catania, Italy
[9]Istituto Nazionale di Fisica Nucleare - Sezione di Napoli, Napoli, Italy
[10]Dipartimento di Fisica Ettore Pancini, Università di Napoli Federico II, Napoli, Italy
[11]Joint Institute for Nuclear Research, Dubna, Russia, and Institute of Nuclear Physics, Tashkent, Uzbekistan
[12]Facoltà di Ingegneria e Architettura, Università Kore, Enna, Italy
[13]Heavy Ion Laboratory, University of Warsaw, Warsaw, Poland
[14]Faculty of Physics, University of Warsaw, Warsaw, Poland
[15]Dipartimento di Fisica e Astronomia, Università G. Galilei and INFN-Sezione di Padova, Padova, Italy

Abstract. The study of nuclei properties and of collision dynamics is a very active research field whose result have implications in different domains as for example astrophysics. The present and future facilities delivering radioactive ion beams with high intensity allow to extend these studies in the region far from the stability valley. New insight has thus been found on the effects of neutron richness on reaction mechanisms as well as on nuclear structure and nuclear matter properties, as for instance, the role of symmetry energy term of the nuclear Equation of State. The presence of diverse reaction products demands for highly performing and very specialized devices, also able to disentangle among different mechanisms, from fast dynamical processes to statistical emission from equilibrated sources. Numerous studies of the effects of N/Z ratio on fusion and associated processes can be found at different energies, together with many examples of the influence of neutron richness on the reaction time scale and the competition between equilibrated and prompt processes. A survey of very recent findings obtained with the CHIMERA and FARCOS devices is presented.

1 Physics of isospin in nuclear reactions

Heavy ion collisions are a powerful instrument to study nuclear matter characteristics under off-equilibrium conditions. One important item among the different open questions addressed with these studies is the study of the characteristic of the equation of state of nuclear matter, and in particular of its symmetry energy term E_{sym}. This term, related to the N/Z of the system and whose behaviour far from normal nuclear density is still quite unknown, can affect many processes.

Some examples at sub-saturation density are given by the multifragmentation, the isospin diffusion towards equilibration in N/Z between two reaction partners, the isospin distillation with neutron enrichment associated with a possible liquid-gas phase transition, as well as the clustering at low density and the vaporization (cluster mixing with nucleon gas). At supra-saturation density one can mention the nucleon elliptic flow at high transverse momentum and the π^-/π^+ and K^-/K^+ production ratios.

The development of radioactive beams at various energies in different laboratories surely open new scenario and possibility to study very asymmetric nuclear matter.

The interest is of course extended in other research fields, providing also some other constraints on symmetry energy as a function of the baryonic density $E_{sym}(\rho)$. In the astrophysics domain, neutron star structure, size and mass, crust/core transition, stellar explosion and nucleosynthesis are all strongly affected by this term. The characteristic of nuclear structure, with the properties of nuclei near drip-lines, nucleon skin and halo, as well as all the behaviour of collective vibrations (GDR, PDR), are widely studied to obtain information on this term.

In this work, we present a survey of some recent results obtained on these topics with the detectors

* Corresponding author: giuseppe.politi@ct.infn.it

CHIMERA and FARCOS. The devices are illustrated in Sec. 2, Section 3 reports on the effects of isospin on competition between dynamical and statistical fission of the quasi-projectile, Section 4 shows the observed effects of isospin on compound nucleus formation and decay while Section 5 presents the results of the study of pigmy dipole resonance in a neutron rich nucleus.

2 Experimental devices

The analysis of the characteristics of the reaction products arising from aforementioned nuclear collisions demands very performing experimental devices. Event selection and reconstruction and reaction mechanism characterization can be obtained only with highly efficient device, also allowing the particle identification and the measurement of kinematic quantities.

The CHIMERA multidetector [1-4] has been extensively working with this purpose in the last two decades at Laboratori Nazionali del Sud in Catania, proving its capabilities to provide accurate results in the intermediate energies regime (E = 10-100 MeV/nucleon) collisions characterized by final states with a large number of charged products that populate a broad energy range.

The device consists of 1192 Silicon - Cesium Iodide thallium doped CsI(Tl) telescopes, covering the 94% of the total solid angle, and employing different techniques to identify reaction products. Particles punching through the silicon detectors were identified in charge, with also isotopic identification for light fragments ($Z \leq 9$), by using the ΔE-E technique. Light charged particles of atomic numbers $Z \leq 2$ were isotopically identified by the pulse shape analysis (fast-slow technique) of CsI(Tl) signals. Direct velocity measurement for ions of $Z > 2$, and information on the mass number of heavy particles stopped in silicon detectors, were obtained via the Time-of-Flight (TOF) technique. Slow moving particles, stopped in the silicon detectors, were also identified in charge via a pulse shape discrimination, based on energy-rise time correlation. This latter technique, realized with the implementation of a specifically performed electronic tool [4], extended the operative domain of the array at lower bombarding energy (E < 10 MeV/nucleon).

In some case a very high angular resolution can be mandatory in order to reconstruct the reaction kinematics and to study the correlation among the reaction products, providing a powerful method to investigate on space and time properties of the studied collisions. The FARCOS array [5, 6], presently under construction, will consist of a modular array of 20 triple telescopes, each of them constituted by two stages of DSSSD 300 and 1500 μm thick, followed by four CsI(Tl) scintillators read by a photo-diode. Thanks to the modular structure, shown in one possible configuration in Fig. 1, the covered angular range can thus be adapted and a very high angular resolution can be obtained. A fully digital acquisition will be used, coupled to a on-purpose realized front end electronics, whose good performances were tested during many in beam experiments.

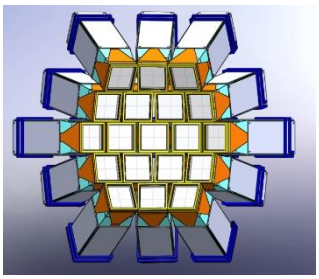

Figure 1. Artistic view of 20 modules of FARCOS array in a possible configuration.

3 Isospin influence on dynamical emission of fragments from quasi projectile

In heavy-ion collisions at Fermi energies the production of light particles and heavier fragments can be due to different reaction mechanisms related to various time scales [7–18]. As an example, in semi-peripheral collisions the coexistence of light fragments emission from prompt neck- fragmentation process [7, 8, 10–12, 15, 16], projectile-like fragments collinear massive break-up [9, 11, 13, 14, 19, 20] and equilibrated projectile binary fission-like emission [13, 16, 19, 20] has been reported within the same range of large relative impact parameters. Thus, within a limited range of entrance conditions of relative energy and angular momenta, the competition among mechanisms with very different time scales, from prompt Intermediate Mass Fragments (IMFs) emissions (tens of fm/c) to equilibrated decay (≫ 300 fm/c), has been noticed. This triggers for further investigations in order to understand the roles played by the entrance properties of the systems, the isospin (N/Z) degree of freedom as well as the system size, in triggering the aforementioned reaction mechanisms, thus affecting their cross sections.

This work aims to show a physics case in which the isospin degree of freedom can influence the reaction path, affecting the occurrence or not of dynamical processes. In fact, in a previous work [20], we studied the IMFs emission in semi-peripheral collisions of neutron rich $^{124}Sn+^{64}Ni$ and neutron poor $^{112}Sn+^{58}Ni$ systems at the beam energy of 35 A·MeV. The dynamical (prompt) IMFs emission was proved to be more probable for the neutron rich system. We found that the IMFs statistical-equilibrated binary fission-like emission was equally probable for the two systems, while the dynamical splitting was favoured for the neutron rich system, especially for heavier IMFs. Since the atomic numbers are equal (for both projectile and target) in the two Sn+Ni systems, the enhancement of the dynamical emission in the neutron rich system was mainly ascribed to the different N/Z ratio, indicating an entrance channel Isospin effect. Nevertheless, at that stage, a possible influence of the mass difference (A=188 vs A=170) could not be excluded. For this reason, in order to disentangle genuine entrance channel Isospin effects from a possible influence of system size, we carried out a new experiment, using the $^{124}Xe+^{64}Zn$ system, a projectile/target combination having

the same mass as the neutron rich ^{124}Sn +^{64}Ni system and a N/Z near to the value of the neutron poor ^{112}Sn+^{58}Ni one, at the same bombarding energy of 35 A·MeV.

The data were collected at the INFN-LNS in Catania by using the CHIMERA multi-detector [1-4] in order to detect and identify the reaction products. A beam of ^{124}Xe bombarded ^{64}Zn (308 μg/cm^2) target and events were registered when at least 2 charged particle hits in the CHIMERA silicon detectors.

In order to disentangle dynamical and statistical emissions and evaluate their probabilities, we applied the analysis method already used in [20] and there fully described. Semi-peripheral events and fragments coming from projectile emission were selected by selected cuts on correlation plots of size vs parallel velocity of detected particles. The dynamical and statistical components were measured by looking at the cos(θ_{prox}) distribution, where θ_{prox} is the angle between the breakup axis, oriented from the light to the heavy fragment of the primary Projectile break up, and the recoil velocity in the centre of mass reference of the projectile. The ratio of the dynamical component to the total contribution (dynamical + statistical) is shown in Fig. 2, as a function of the atomic number Z of the fragment, for the three systems.

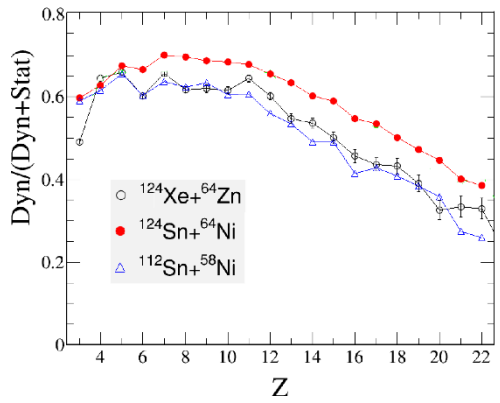

Figure 2. Ratio of the dynamical component to the total (dynamical + statistical) value as a function of the fragment atomic number Z, for the ^{124}Xe+^{64}Zn (empty circles), the ^{124}Sn+^{64}Ni (full circles) and ^{112}Sn+^{58}Ni (empty triangles) systems.

From the results of the three systems, it follows that dynamical IMFs emission probability grows with the N/Z content of, both, target and projectile. Clearly, this agrees with the results for the two Sn+Ni systems, already seen in [14], where Isospin content of both projectile and target changes; however this couple of systems, having the same Coulomb effects, allowed us to suggest, in the previous mentioned work [20], that the observed differences in dynamical IMFs emission probability had to be triggered by size or Isospin difference; now, the present analysis on isobaric systems excludes, within the experimental accuracy, substantial size effect in the investigated reactions.

A further quantitative analysis [21] found that the increase of the Dynamical emission probability with the isospin of the entrance channel is twice more sensitive to the target (N/Z) content with respect to the projectile one.

4 Effect of isospin on compound nucleus formation and decay

In the field of heavy ion collisions at low energy (E/A < 10-15 MeV/nucleon) one of the most studied mechanism is the fusion reaction, with the compound nucleus (CN) formation and its following decay modes. Actually, fundamental aspects of nuclear matter can be studied by means of this mechanism, allowing the formation of nuclei in extreme condition of spin and temperature. Furthermore, in this energy domain, one may expect the rising of other mechanisms in which not all the degrees of freedom are equilibrated. In this framework, the isospin of the systems created in the studied reactions, closely related to the isotopic ratio N=Z, is expected to play a fundamental role and on the fragments production and on the emission process [22-25]. For this reason, we investigated the competition among the various fragments production modes in the reactions ^{78}Kr+^{40}Ca (neutron poor system) and ^{86}Kr+^{48}Ca (neutron rich system), studied with the CHIMERA device [1-4] at laboratory energy of 10 MeV/nucleon [26-28]. Reaction product identification was obtained as detailed in the previous section, with an enhancement in the use of time of flight and pulse shape analysis in silicon detector [4] due to the lower energy of the fragments, mainly stopped in the first stage of the CHIMERA telescope.

Mass distributions at different angles and correlations between emitted fragments have been used to qualitatively study the diverse reaction mechanisms and the differences in their relative contributions due to the isospin of the two systems. As an example the complete event selection, global decay patterns can also be studied in Fig. 3, where the mass A versus the parallel velocity V_{par} is reported for each reaction product and for the two studied systems, for well detected events.

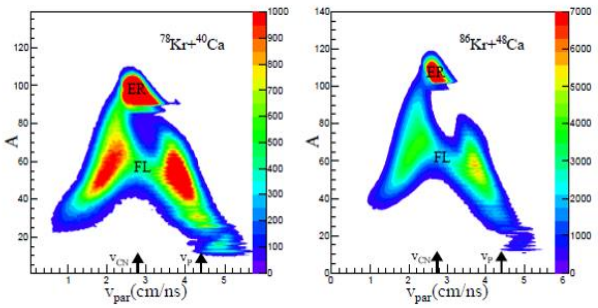

Figure 3. Mass versus parallel velocity for reaction products detected in complete events for the two systems; the arrows indicate compound nucleus (V_{CN}) and projectile velocity (V_P).

We can disentangle the fragments coming from the different decay modes of the composite system formed in the reactions, as the Evaporation Residues (ER) centred around the compound nucleus velocity V_{CN} and the Fission-Like fragments (FL) distributed along the two branches coming from the corresponding possible kinematic solutions. From the comparison it seems that the FL process is more pronounced in the neutron poor system. Velocity spectra, total kinetic energies and angular distribution of the fragments indicate a high

degree of energy relaxation of the system formed in the collision before the breakup. Heavier residues characteristics are compatible with their production via an evaporation process following complete and incomplete fusion of the two partners. On the top of these mechanisms a binary process not completely relaxed in mass asymmetry has been observed, giving a stronger yield at forward angles in the angular distributions of heavier fragments.

Production cross section of each element has been measured from the angular distributions, showing charge distributions asymmetric with respect to the expected value for symmetric fission, probably because of an aforementioned not equilibrated process. Staggering effects are also evident in the charge distributions of fragments with $Z < 17$, more pronounced for neutron poor system, and a higher fragment yield is globally measured for the neutron rich one.

Some differences in charge distributions have also been observed with respect to the neutron poor system studied at lower energy in a previous experiment [29], suggesting different mechanisms and contributions to the reaction cross section as a function of energy. In particular, at lower energy evaporation is the favoured decay mode while at higher energy the fusion-fission channel prevails.

The single values of fragment production cross section have thus been used to reconstruct the total cross section of each reaction mechanism in both systems, in order to look for differences due to the N/Z degree of freedom. The results [28] show that neutron enrichment seems to discourage the fusion process and limiting at the same time the fission decay process.

Experimental fragment production cross sections were compared with predictions [29, 30] obtained by using the dynamical Dinuclear System (DNS) model and the statistical code GEMINI++, using different values for the maximum angular momentum and excitation energy.

Calculations made with the DNS seem to reproduce the general trend of charge distribution but do not give very satisfactory quantitative results in terms of cross section for fragment production for both systems; the calculated yields are globally lower than the experimental ones, probably due to some underestimation of maximum angular momentum involved in the reactions.

Predictions of GEMINI+, made initially with the same J_{max} of DNS, are quite different from these latter for heavier fragments; moreover, they strongly differ from experimental results of neutron rich system for light elements showing the possible occurrence of a non-statistical decay mode of ^{134}Ba* that is not accounted for in the code.

Both calculations performed with the value of J_{max} assumed by the DNS model underestimate the experimental production cross sections, with the DNS model reproducing slightly better the ratio between ER and FL contributions, due to expected contribution of quasi-fission events. GEMINI++ results obtained with a higher value of J_{max}, related to the experimental fusion cross sections, present globally higher values of the fragments yields, with essentially the same ratio between different process contributions.

5 Study of pigmy dipole resonance

The so-called Pygmy Dipole Resonance (PDR) has been predicted to be present in all the nuclei with neutron excess, in particular, for those far from the stability line. In fact, it has been shown that, as soon as the number of neutrons increases, the isovector and isoscalar dipole responses show a small bump at low energy in the strength distribution, which is well separated from the well-known peak of the Giant Dipole Resonance (GDR). This mode has a strong relation with the symmetry energy and it has been used as a further tool to constrain it. Assuming that a nucleus with a neutron excess is formed by a saturated core, with the same number of neutrons and protons, and a neutron skin, the PDR can thus be considered as a surface mode associated with the motion of the neutron skin against the saturated core. This mode can be populated by both isoscalar and isovector probes [31].

Several experiments have been performed on stable nuclei revealing a particular property known as" isospin splitting" [32-34]: only the low energy region of the PDR is populated by both isoscalar and isovector probes, while the higher part is excited mainly via electromagnetic interaction. It is interesting to investigate whether the same effect is observed also for the PDR region above the neutron emission threshold and for unstable nuclei, as already done for example at the GSI, using relativistic Coulomb excitations on ^{132}Sn [35] and ^{68}Ni [36, 37] isotopes.

We report here on the first observation of the PDR above the neutron emission threshold, in the ^{68}Ni nucleus, using an isoscalar probe, obtained in an experiment carried out at INFN-LNS of Catania. A ^{70}Zn primary beam was accelerated to an energy of 40A MeV, using the Superconducting Cyclotron (CS), and it impinged on a 250 μm thick ^{9}Be target to produce, with a projectile fragmentation reaction, the ^{68}Ni beam, delivered via the FRIBs@LNS fragment separator of the INFN-LNS [38, 39]. In such a facility, a tagging system was used in order to event by event characterize the cocktail beam [40]. A ^{12}C target, 75 μm thick, was used to induce the isoscalar excitation on the projectile nucleus. The scattered ^{68}Ni ions were detected and identified in four telescopes of the FARCOS array [5, 6] placed just after the sphere of the CHIMERA multidetector [1, 4] and covering angles from 2° to 7°, with approximately 70% coverage of azimuthal angles. The γ-rays from the PDR decay were detected using the CsI(Tl) scintillators of the CHIMERA multidetector sphere, details on their detection and identification can be found in refs. [41-42]. The energy calibration of CsI(Tl) detectors was performed using 24 MeV proton elastic and inelastic scattering on ^{12}C, ^{197}Au and CH_2 targets. More in detail scattering of protons and pulser signals were used to calibrate all detectors in proton equivalent energy, verifying the linearity of the response function. The proton energy calibration was converted in γ-ray energy calibration using, as a reference point, the decay of the 4.44 MeV level of the ^{12}C.

The Doppler shift corrected γ-ray energy spectrum was measured in coincidence with the Ni fragments detected by the FARCOS array. The experimental data

were compared with calculations performed using the statistical code DCASCADE folded with the CsI(Tl) response function, evaluated by performing Geant4 simulation. A good agreement was obtained only including resonances and in particular a PDR contribution with a centroid around 10 MeV, a width of 2 MeV and a strength of 9 % ± 2 % EWSR, a GDR contribution with a centroid of 17 MeV, a width of 6 MeV and a strength of 91 % ± 2 % EWSR and a GQR with a centroid around 16 MeV and a width of 1.5 MeV. The parameters of the PDR and GDR are in reasonable agreement, inside our error bars, with the values reported in Ref. [37].

Due to the energy resolution of CsI(Tl) detectors the population of the PDR in these data was put in evidence only by a small change of slope around 10 MeV and by the comparison with statistical calculations. A better experimental evidence of the PDR population can be obtained by comparing the energy spectra of γ-rays emitted in coincidence with the ^{68}Ni channel and with ^{66,67}Ni channels. In fact, at this low excitation energy the high energy γ-decay of the PDR hinders further particle decay. On the contrary, if one or more neutrons are emitted by the system, the high energy γ-rays decay is inhibited. For these reasons we compare the γ-rays energy spectrum (black dots) in coincidence with the ^{68}Ni with the one measured in coincidence with neutron decay channels ^{66,67}Ni, as shown in Fig. 4 (adapted from [43]).

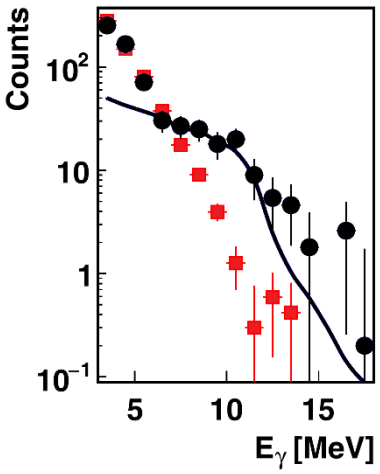

Figure 4. γ-ray energy spectra Doppler shift corrected. The black dots represent the coincidence with ^{68}Ni, the red squares the ones with ^{66,67}Ni. The full line is the γ-rays first step spectrum obtained with CASCADE (see text).

The two spectra are normalized in the low energy region. We note the enhancement around 10 MeV, as it was expected, due to the PDR decay in the ^{68}Ni channel. We observe a relatively small yield in the GDR high energy region as predicted by the semi-classical calculations. Indeed, these calculations show that, at these relatively low incident energies and with the low Coulomb field of the target, the excitation probability for the PDR mode is higher than the one corresponding to the GDR energy region. The small yield is however also due to the lower detection efficiency in the higher energy region.

One can compare the γ-rays spectrum in coincidence with ^{68}Ni with γ-rays first step spectra generated with CASCADE, namely with the ones emitted as first particle in the decay process. In fact, such events at the low excitation energy of the system produce only ^{68}Ni nuclei. This calculation, folded with the CsI(Tl) response function, is plotted as full line in Fig. 4. The comparison is quite good and the calculation reproduces the bump in the energy region of the PDR. Clearly, in this calculation, the lower energy spectrum is not reproduced because in this energy region the contribution of the decay of discrete levels in the final decay steps is missing.

It is very important to verify the *E1* character of the observed bump at around 10 MeV in coincidence with the ^{68}Ni channel, in order to prove the dipole character of the transition. The angular distribution of the emitted γ-rays in the region of the enhancement at around 10 MeV was measured, and data were corrected for the effective γ-ray detection efficiency of different type of CHIMERA CsI(Tl), evaluated using Geant4 simulation at 10 MeV. Notwithstanding the scarce statistics, due also to the reduced angular resolution of the sphere of CHIMERA detector, the results shows the typical distribution expected for a dipole transition with a maximum around 90° [43].

Being sure of the *E1* character of the resonance we can compare the measured γ-ray spectrum to the one obtained using an almost pure isovector probe, like in the relativistic Coulomb excitation in Ref. [36], observing that there is almost an order of magnitude difference between the two cross sections, probably due to the different reactions regimes. Within the small statistics and the relatively scarce energy resolution of the present measurement and previous experiments this comparison seems to indicate that the outcome of the excitation process due to the two isoscalar and isovector probes is similar along the PDR energy region. Therefore, the isospin splitting seems not to be observed at the energy above the neutron emission threshold; however more precise measurements are necessary to better prove this observation.

6 Conclusions and perspectives

Isospin of participants can strongly affect reaction mechanisms in heavy ion collisions, whose study can provide information about some fundamental characteristics of the equation of state, in particular for asymmetric nuclear matter. New scenarios are opening thanks to the development in the last decades of many facilities providing radioactive beams with sufficiently high current and at different energies.

The CHIMERA and FARCOS detectors, operating at LNS-INFN in Catania, are two powerful devices allowing for a detailed study of reaction products characteristics and the extraction of information about the involved reaction mechanisms. Some examples of the obtained results have been presented.

The competition between dynamical and statistical fission of quasi projectile was studied in systems with different N/Z, providing information on some parameters

of the EOS. New measurements at lower energy are in program in order to explore the evolution of the phenomenon with this parameter.

The dependence of compound nucleus formation and decay processes on N/Z of the systems was investigated by comparing fragment production yields and the cross sections of different processes in two systems differing for neutron population. New experiments will be done with radioactive beams to push towards neutron richer systems.

A first study of PDR in ^{68}Ni with an isoscalar probe was accomplished, allowing the study of this excitation mode in unstable nuclei; results seems to confirm that the isospin splitting is not observed at the energy above the neutron emission threshold. Further and more refined experiments with isovector and isoscalar probes are foreseen.

References

1. A. Pagano *et al.,* Nucl. Phys. A **734**, 504 (2004)
2. A. Pagano, Nucl. Phys. News **22**, 28 (2012)
3. E. De Filippo and A. Pagano, Eur. Phys. J. A **50**, 32 (2014)
4. M. Alderighi *et al*., Nucl. Instr. Meth. A **52**, 1624 (2005)
5. E. V. Pagano *et al*., EPJ Web of Conf. **117**, 10008 (2016)
6. L. Acosta *et al.,* J. Phys.: Conf. Ser. **730**, 012001 (2016)
7. A. Pagano *et al*., Nucl. Phys. A **734**, 504 (2004)
8. E. De Filippo *et al*., Phys. Rev. C **71**, 044602 (2005)
9. E. De Filippo *et al*., Phys. Rev. C **71**, 064604 (2005)
10. M. Di Toro, A. Olmi, and R. Roy, Eur. Phys. J. A **30**, 65 (2006)
11. M. Papa *et al*., Phys. Rev. C **75**, 054616 (2007)
12. S. Piantelli *et al*., Phys. Rev. C **76**, 061601 (2007)
13. P. Russotto *et al*., Phys. Rev. C **81**, 064605 (2010)
14. A. McIntosh *et al*., Phys. Rev. C **81**, 034603 (2010)
15. E. De Filippo *et al*., Phys. Rev. C **86**, 014610 (2012)
16. E. De Filippo and A. Pagano, Eur. Phys. J. A **50**, 32 (2014)
17. A. Rodriguez Manso *et al*., Phy. Rev. C **95**, 044604 (2017)
18. A. Jedele *et al*., Phys. Rev. Lett. **118**, 062501 (2017)
19. F. Bocage *et al*., Nucl. Phys. A **676**, 391 (2000)
20. P. Russotto *et al*., Phys. Rev. C **91**, 014610 (2015)
21. P. Russotto *et al*., submitted to Eur. Phys. J. A
22. G. Cardella *et al*., Phys. Rev. C **85**, 064609 (2012)
23. K. Godbey, A. S. Umar, and C. Simenel, Phys. Rev. C **95**, 011601 (2017)
24. I. Lombardo *et al*., Phys. Rev. C **84**, 024613 (2011)
25. P. Russotto *et al*., Phys. Rev. C **91**, 014610 (2015)
26. M. La Commara *et al*., EPJ Web of Conf. **66**, 03052 (2014)
27. B. Gnoffo, Il Nuovo Cimento **39** C, 275 (2016)
28. S. Pirrone *et al*., submitted to Eur. Phys. J. A
29. G. Ademard *et al.,* Phys. Rev. C **83**, 054619 (2011)
30. Sh.A. Kalandarov *et al*., Phys. Rev. C **93**, 024613 (2016)
31. E. G. Lanza *et al*., Phys. Rev. C **84**, 064602 (2011)
32. N. Paar *et al*., Rep. Prog. Phys. C **70**, 691 (2007) and references therein
33. D. Savran *et al*., Progr. Part. Nucl. Phys. **70**, 210 (2013)
34. A. Bracco *et al*., Eur. Phys. J. A **51**, 99 (2015) 99
35. P. Adrich *et al*., Phys. Rev. Lett. **95**, 132501 (2005)
36. O. Wieland *et al*., Phys. Rev. Lett. **102**, 092502 (2009)
37. D. M. Rossi *et al*., Phys. Rev. Lett. **111**, 242503 (2013)
38. https://www.lns.infn.it/it/acceleratori/fribs-lns.htm, 2018
39. G. Raciti *et al*., Nucl. Instr. Meth. B **266**, 4632 (2008)
40. I. Lombardo *et al*., Nucl. Phys. B (Proc. Suppl.) **215**, 272 (2011)
41. M. Alderighi *et al*., Nucl. Instr. Meth. A **489**, 257 (2002)
42. G. Cardella *et a*l., Nucl. Instr. Meth. A **799**, 64 (2015)
43. S. Martorana *et al*., Phys. Lett. B **782**, 112 (2018)